Thermal conductivity of low-particle-concentration suspensions: Correlation function approach

Leonid Braginsky[1,2,*] and Valery Shklover[1]
[1]*Laboratory of Crystallography, Department of Materials, ETH Zurich, 8093 Zurich, Switzerland*
[2]*Institute of Semiconductor Physics, 630090 Novosibirsk, Russia*
(Received 3 August 2008; published 22 December 2008)

A method of determining the thermal conductivity of nanofluids is proposed. The approach uses the two-point correlation function of local thermal conductivities, which can be estimated from an optical image of the fluid. The effect of the particles shape and their agglomeration on the thermal conductivity of nanofluids is investigated. Effective increase in the particles concentration due to ordering at the nanoparticle-liquid interface is considered. It is shown that the effective media approximation holds for nanofluids with a low volume fraction of nanoparticles.

DOI: 10.1103/PhysRevB.78.224205 PACS number(s): 65.80.+n, 65.20.−w, 44.35.+c, 66.25.+g

I. INTRODUCTION

Some nanofluids, i.e., stable suspensions of solid nanoparticles, were found to show anomalously high thermal conductivity (compared to that of the base fluids) at very low volume fractions of nanoparticles.[1–4] To explain this enhancement, the microconvection mechanism due to Brownian motion has been suggested.[5,6] The model predicts deviation from the classical Maxwell effective-medium theory.[7] Other experiments, however, do not exhibit considerable deviation from the effective-medium theory.[8,9] This conclusion has been confirmed by molecular-dynamics simulations.[10] It seems that the microconvection is significant only at small ($<0.5\%$) volume fractions of nanoparticles.[11]

A nonlinear relationship between thermal conductivity and volume fraction of nanoparticles,[12] as well as strong temperature-dependent and nanoparticle-size-dependent thermal conductivities has been observed.[4,13,14] The latter also contradicts the effective-medium model.

Light scattering and viscosimetry studies verify that nanoparticles in nanofluids are often aggregated.[12,13,15,16] A typical aggregation of colloidal silica beads is presented in Fig. 1. The aggregates have multimodal size distribution, time-dependent particle size distribution, and a correlation is observed between the changes in the size distribution and the measured thermal conductivity and viscosity.[13,17]

Maxwell's effective-medium model[7] is the first analytical estimation of the thermal conductivity of nonhomogeneous media. It has been generalized in number of works (see, e.g., Ref. 18 and 19). Digital imaging allows numerical treatment of the problem. The paper[20] suggests numerical solution of the heat-flow equation with the finite difference mesh directly imposed to the image. The main shortcoming of this approach comes from the two-dimensional (2D) character of the solution. Rough estimation of the error can be found by comparing the three-dimensional (3D) and 2D analytical solutions. The error is about $p/6$, where p is the volume fraction of nanoparticles, for the spherical particles, but it can be essentially larger for the elongated ones.

This paper suggests a different way of using digital images for the estimation of thermal conductivity. Unlike Ref. 20, we use the images only to calculate the two-point correlation function of the local thermal conductivities, which then can be used to estimate the effective thermal conductivity of the nanofluid. Symmetry of the fluid flux allows us to consider the three-dimensional problem using the two-dimensional digital image.

It should be noted that effective thermal conductivity we considered here is the thermal conductivity of the motionless liquid. To investigate heat transport in the flowing liquid, it is necessary to write the heat-flow equation (with the effective thermal conductivity determined here as the intrinsic value) together with the Navier-Stocks equation.

II. ESTIMATION OF THERMAL CONDUCTIVITY

The temperature T at each point $\boldsymbol{r}$ of a motionless nanofluid obeys the heat-flow equation

$$\frac{\partial T}{\partial t} - \mathrm{div}[\kappa(\boldsymbol{r})\mathrm{grad}\ T] = \delta(\boldsymbol{r},t), \tag{1}$$

where

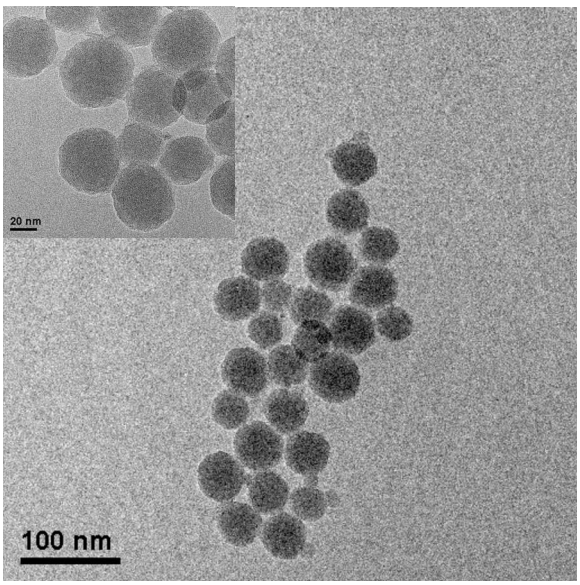

FIG. 1. Aggregate of silica nanoparticles (TEM image recorded with Tecnai F30 at 300 kV acceleration voltage). Amorphous structure of the nanoparticles, low monodispersity, and surface inhomogeneities of the beads can be seen.

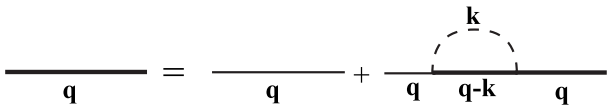

FIG. 2. Diagrammatic expansion for the average temperature in first approximation on the volume fraction of nanoparticles p.

$$\kappa(\boldsymbol{r}) = \begin{cases} \kappa_L & \text{in the fluid,} \\ \kappa_S & \text{in the particles,} \end{cases}$$

and δ is the momentary point heat origin. To introduce the effective thermal conductivity κ_{eff}, we suppose the average temperature satisfies the equation

$$\frac{\partial \bar{T}}{\partial t} - \kappa_{\text{eff}} \text{div grad } \bar{T} = \delta(\boldsymbol{r},t).$$

To find it, we write the local thermal conductivity as the sum of its average κ_0 and fluctuate $\eta(\boldsymbol{r})$ components

$$\kappa(\boldsymbol{r}) = \kappa_0 + \eta(\boldsymbol{r}),$$

where

$$\kappa_0 = \kappa_L(1-p) + \kappa_S p, \quad \overline{\eta(\boldsymbol{r})} = 0,$$

and p is the volume fraction of nanoparticles. Perturbation with respect to $\eta(\boldsymbol{r})$ permits us to study the effect of disorder in terms of the two-point correlation function $S(\boldsymbol{r},\boldsymbol{r}') = \overline{\eta(\boldsymbol{r})\eta(\boldsymbol{r}')}$. For a homogeneous in average particle distribution, this value depends only on the distance $S(\boldsymbol{r},\boldsymbol{r}') = S(\boldsymbol{r}-\boldsymbol{r}')$. This function has maximum at zero $S(0) = \overline{\eta^2(\boldsymbol{r})} = p(1-p)(\kappa_S-\kappa_L)^2$ and vanishes at infinity because fluctuations $\eta(\mathbf{r})$ and $\eta(\boldsymbol{r}')$ are independent then $|\boldsymbol{r}-\boldsymbol{r}'| \to \infty$. Furthermore we will use the normalized correlation function $W(\boldsymbol{r}-\boldsymbol{r}') = S(\boldsymbol{r}-\boldsymbol{r}')/S(0)$. This value is independent of conductivities κ_L and κ_S; it is a function of the nanofluid structure (its composition, distribution of nanoparticles, etc.) only.

The effective thermal conductivity can be determined with the diagrammatic technique for the average temperature.[21] This permits us to find this value as a power series of p, where the expansion coefficients are expressed via the correlation function. To do that, we considered the response of the media on sudden heating by a remote unit point origin. In a homogeneous media such heating results in a temperature increase

$$T(r,t) = \frac{1}{8(\pi\kappa^2 t)^{3/2}} e^{-r^2/4\kappa^2 t}, \tag{2}$$

where r, t, and κ are the distance from the origin, time, and thermal conductivity of the media, respectively. Average temperature increase in a nonhomogeneous media can be found as an expansion in series on the nonhomogeneity. Considering the problem in the Fourier representation, we write the zero and first terms of this series as it is presented in Fig. 2, where the straight lines correspond to the Fourier transform of T

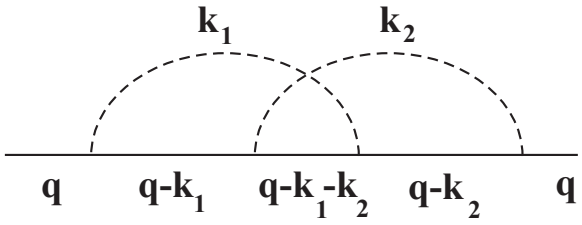

FIG. 3. Second order (p^2) correction to the diagrams of Fig. 2

$$T(\boldsymbol{r},t) = \frac{1}{(2\pi)^4} \int \Theta(\boldsymbol{k},\omega) e^{i(\boldsymbol{kr}-\omega t)} d^3k d\omega.$$

The thin straight lines correspond to the zero approximation [Fourier transform of Eq. (2)]

$$\Theta_0(\boldsymbol{q}) = \frac{1}{\kappa_0 q^2 - i\delta}, \tag{3}$$

$\delta \to +0$, the bold straight lines correspond to the total sum Θ, and the dashed lines to Fourier transforms of the correlation function

$$\tilde{W}(\boldsymbol{k}) = \int W(\boldsymbol{r}) e^{i\boldsymbol{kr}} d^3r$$

multiplied by $S(0) = p(1-p)(\kappa_S-\kappa_L)^2$, the factor $[\boldsymbol{q}\cdot(\boldsymbol{q}-\boldsymbol{k})]$ corresponds to each vertex between $\Theta_0(\boldsymbol{q})$, $\Theta_0(\boldsymbol{q}-\boldsymbol{k})$, and $\tilde{W}(\boldsymbol{k})$. Integration over the inner $\boldsymbol{k}$ vectors [i.e., $d^3k/(2\pi)^3$] is assumed. The wave vectors obey the conservation law at each vertex. This law permits the addition of diagrams in Fig. 2. The result is

$$\Theta = \frac{1}{(\kappa_0 - \Sigma)q^2 - i\delta}, \tag{4}$$

where

$$\Sigma = \frac{(\kappa_S-\kappa_L)^2 p(1-p)}{(2\pi)^3} \int \frac{k_z^2 \tilde{W}(\boldsymbol{k})}{\kappa_0 \boldsymbol{k}^2 - i\delta} d^3k.$$

From comparison with Eq. (3) it follows that

$$\kappa_{\text{eff}} = \kappa_0 - \Sigma \tag{5}$$

is the effective thermal conductivity. The second-order correction to Σ is presented in Fig. 3.

In general, to determine the effective thermal conductivity we have to add all the considerable contributions to Σ and then calculate κ_{eff} from Eq. (5). Apparently, $(\kappa_S-\kappa_L)^2 p(1-p)/\kappa_0^2$ is the actual parameter of perturbation. We can consider only the first diagram (Fig. 2) if $(\kappa_S-\kappa_L)^2 p(1-p)/\kappa_0^2 \ll 1$. Otherwise, the diagrams of higher order have to be taken into account. In particular, this is the case when $\kappa_S p \gg \kappa_L$ so that $\Sigma \sim \kappa_S \sim \kappa_0$.

III. RESULTS OF MODELING

Figure 4 presents the model structures used in the calculations. The first structure (a) consists of primitive round

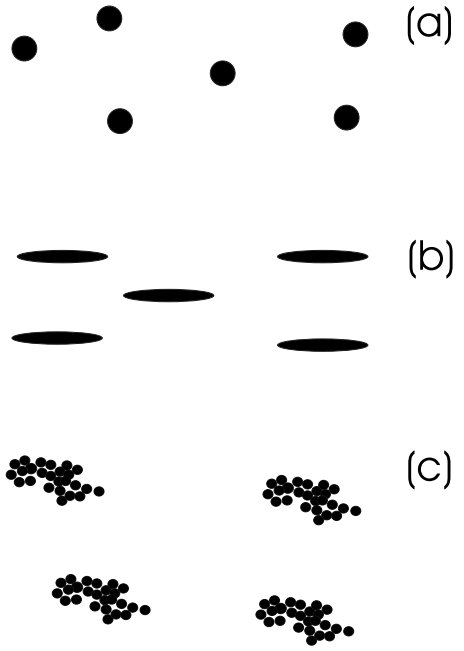

FIG. 4. Schematic of modeled structures: (a) dispersed spherical and (b) elongated particles, and (c) elongated aggregates of spherical particles.

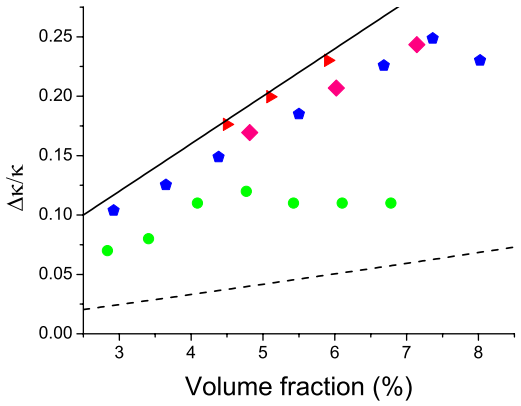

FIG. 5. (Color online) Thermal conductivity vs volume fraction of nanoparticles for the structures of Fig. 4: (a) green circles, (b) red triangles, and (c) blue pentagonals. (b) Pink rhombuses present thermal conductivity of elliptic particles, whose aspect ratio 3:5 is close to that of structure (c). Black straight and dashed lines correspond to the maximal $\kappa_{\max}=p\kappa_S+(1-p)\kappa_L$ and minimal $\kappa_{\min}^{-1}=p\kappa_S^{-1}+(1-p)\kappa_L^{-1}$ bounds, respectively. $\kappa_S/\kappa_L=5$ for all the structures.

nanoparticles. The second one (b) is composed of elliptical particles aligned in the direction of the flow; the aspect ratio of the ellipses is 1:9. The third structure (c) corresponds to an agglomerate of round nanoparticles similar to that of Fig. 1; the typical size of the agglomerates in the direction of the flux is about two times larger than the size across the flux.

To estimate the effective thermal conductivity using the formalism of Sec. II, it is necessary to calculate the correlation functions of the structures. To do that we used files of their black-and-white images in the bitmap (bmp) format. We calculated the product $\eta(\boldsymbol{r}_1)\eta(\boldsymbol{r}_2)$, where $\eta=0$, if the appropriate pixel is black, and $\eta=1$, if this pixel is white. The product has been averaged over the array of random points $\boldsymbol{r}_1$ (we used 100 000 points) of the structure for each $\boldsymbol{r}=\boldsymbol{r}_1-\boldsymbol{r}_2$.

We study the heat propagation from the left to the right of each figure [(a)–(c)]. Changing the number of particles, we can estimate the thermal conductivity of each structure as a function of the volume fraction of nanoparticles. Figure 5 presents the results.

To analyze them, let us begin with a one-dimensional structure of the alternate liquid and solid regions, whose thermal conductivities are κ_L and κ_S. Analogous to an electric circuit in which two types of resistors are connected in series, we can estimate the thermal conductivity as

$$\kappa_{\min}^{-1}=p\kappa_S^{-1}+(1-p)\kappa_L^{-1}. \tag{6}$$

The one-dimensional character of estimation (6) indicates an absence of heat flux across the current. To take this flux into account, resistors connected in parallel must also be included. Assuming that such resistors efficiently shunt all κ_S^{-1} in a three-dimensional structure, we can estimate thermal conductivity as

$$\kappa_{\max}=p\kappa_S+(1-p)\kappa_L. \tag{7}$$

Estimations (6) and (7) are the lower and upper limits for thermal conductivity. More accurate estimations of these limits have been done in Ref. 22 using a correlation function approach. Both estimations are presented with bold and dashed lines in Fig. 5.

Figure 5 allows us to understand the influence of the particles shape and their agglomeration on thermal conductivity. We see that model (b) of elongated particles (elliptical particles whose aspect ratio is 1:9) yields thermal conductivity close to upper limit (7). To some extent, this also concerns elongated agglomerates of the round particles (c). Thus, alignment of the nonspherical particles along the liquid flux leads to an appreciable increase in thermal conductivity in this direction.

From Fig. 5 it is clear that the thermal conductivity of nanofluids with (c) agglomerated particles and (d) elliptical particles are nearly equal if their aspect ratios are close. Thus, the volume fraction of nanoparticles and their characteristic aspect ratio are the main parameters determining the thermal conductivity. This is in agreement with the results of the molecular-dynamics simulations.[23] This means also that analytical calculation,[24] where the effect of elliptic particles and their orientation was investigated, can be used for estimation of thermal conductivity of the nanoliquids with the agglomerated particles of small volume fraction (linear parts of the curves in Fig. 5).

Analyzing the dependence of thermal conductivity on the volume fraction of nanoparticles, we find that the effective media approximation works well at small volume fractions. Deviation from this approximation that occurs at larger volume fraction comes from the higher order diagrams (Fig. 3). Roughly, they are important when $p \gtrsim \kappa_S/\kappa_L$. The contribution of the diagrams in Fig. 3 depends on the particle shape: it is smaller for the elongated particles. This increases the range of applicability of the effective media approximation. Note that diagrams of higher order than that presented in

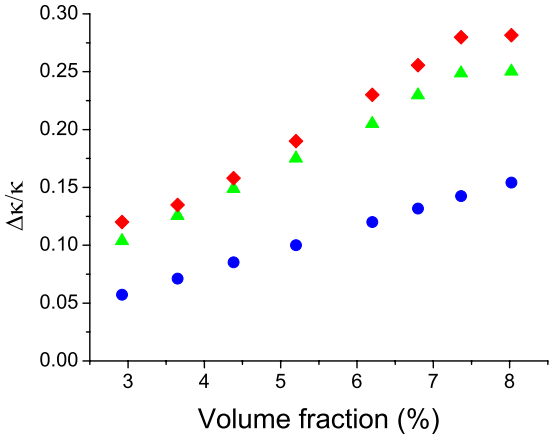

FIG. 6. (Color online) Thermal conductivity vs particle volume fraction for the structure (c) of Fig. 4 for particles of different thermal conductivities: $\kappa_S/\kappa_L=3$ (blue circles), $\kappa_S/\kappa_L=5$ (green triangles), and $\kappa_S/\kappa_L=7$ (red diamonds).

Fig. 3 have not been taken into account in our estimations.

Figure 6 shows the dependence of thermal conductivity on the particle volume fraction for the same structure (c), but different thermal conductivities of the particles from which they are composed. We found a natural increase in thermal conductivity of the nanofluid with an increase in the particle's thermal conductivity. However, this increase is not so prominent for the high-conductive nanoparticles. Moreover, the range of the effective media approximation decreases for the high-conductive nanoparticles. The reason is easy to understand from the electric circuit analogy. Shunting due to the transitioning to the third dimension is not so efficient for resistors of small resistivity. Therefore, the problem becomes close to that of the one-dimensional one with a lower limit estimation of thermal conductivity (6).

Apparently, the heat transport between nanoparticles and the solvent is determined by the character of interfaces between them. Namely, some kind of structure order at the particle/liquid interface occurs. As the result, the thermal conductivity of the liquid at the interface becomes comparable to that of the solid.[25]

To consider this effect assume existence of some intermediate layer where the thermal conductivity κ_i changes continuously between thermal conductivity of the liquid κ_L and the solid κ_S (Fig. 7). For a thin intermediate layer the problem can be reformulated in terms of the boundary conditions

$$T_L - T_S = \frac{\xi}{\tilde{\kappa}_i}\kappa_S \frac{dT_S}{dx}\bigg|_{x=0},$$

where

$$\frac{1}{\tilde{\kappa}_i} = \frac{1}{\xi}\int_0^{\xi} \frac{dx}{\kappa_i(x)},$$

$$\kappa_S \frac{dT_S}{dx}\bigg|_{x=0} = \kappa_L \frac{dT_L}{dx}\bigg|_{x=\xi}. \tag{8}$$

Equations (8) have been obtained after integration of the heat-flow equation over the intermediate region ξ. Nonzero

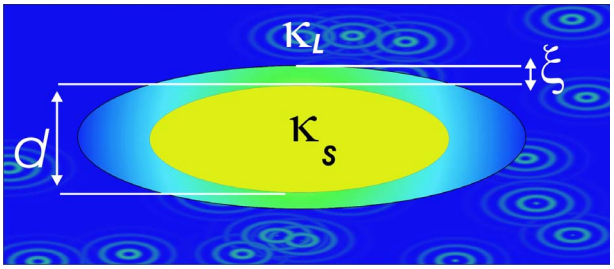

FIG. 7. (Color online) Intermediate layer around the particle

right part of the first Eq. (8) distinguishes it from the commonly used one. Nevertheless, we can find some plane $x=\delta$ near the boundary $x=0$, where the common used boundary condition $T_L(\delta)=T_S(\delta)$ holds. Indeed, expanding the temperatures $T_L(\delta)$ and $T_S(\delta)$ at the vicinity of boundary, we find

$$\delta = \frac{1-\kappa_L/\tilde{\kappa}_i}{1-\kappa_L/\kappa_S}\xi. \tag{9}$$

This means effective increase in the particle size (and so their effective concentration) which should be taken into account in modeling. The effect is proportional to $S\delta$, where S is the lateral area of nanoparticles; it is most important for the nonspherical nanoparticles such as carbon nanotubes.

Effective increase in the particle size due to interfacial layering has been proposed in Ref. 26. However, molecular-dynamics simulations[27] did not find any significant effect on thermal conductivity. Estimation (9) shows that effect, if it exists, can be described by one adjustable parameter δ, which is independent of the particle size and shape. It is the characteristic of the materials of the particles and solvent, which can be measured in experiments for each particle-fluid pair of materials.

In conclusion, we used the correlation function technique to estimate thermal conductivity of nanofluids. The method permits consideration of the real nanofluids, and not only the model structures considered herein. It is shown that the shape of the nanoparticles as well as their agglomeration appreciably influence the thermal conductivity of nanofluids. This effect is due to the alignment of elongated particles along the flux. We found that the thermal conductivity of nanofluids substantially depends only on the volume fraction of nanoparticles and their characteristic aspect ratio.

Alignment of the particles along the flux can occur even in the absence of fluid movement due to the applied pressure difference. Then alignment is due to convection caused by the applied temperature difference. The effect is similar to the chain force due to molecular alignment arising in some polymers under external mechanical[28,29] or thermal[30] stress. This results in an increase in thermal conductivity in the direction of the heat flux.

Ordering of the fluid at the particle boundary results in an effective increase in the particle size, which is more pronounced in the case of small particles. Dependence of the thermal conductivity on the particle's size, which has been observed in some experiments,[4,13,14] can be caused by this effective increase. The thickness of the corresponding intermediate layer is the same for each pair of particle-fluid ma-

terials and can be measured in experiments. It should be noted that the presented consideration concerns only nanoparticles large enough to be characterized by their intrinsic thermal conductivity. Further decrease in the particle size affects the mechanism of the phonon and heat propagations and, thus, can affect not only thermal conductivity, but also viscosity of the fluid. This is the subject of further investigations.

*leonid.braginsky@mat.ethz.ch

[1] J. A. Eastman, S. U. S. Choi, S. Li, W. Yu, and L. J. Thompson, Appl. Phys. Lett. **78**, 718 (2001).
[2] S. K. Das, N. Putra, P. Tiesen, and W. Roetzel, ASME J. Heat Transfer **125**, 567 (2003).
[3] H. Patel, S. K. Das, T. Sundararajan, A. S. Nair, B. Gorge, and T. Pradeep, Appl. Phys. Lett. **83**, 2931 (2003).
[4] J.-H. Lee, K. S. Hwang, S. P. Jang, B. H. Lee, J. H. Kim, S. U. S. Choi, and C. J. Choi, Int. J. Heat Mass Transfer **51**, 2651 (2008).
[5] R. Prasher, P. Bhattacharya, and P. E. Phelan, Phys. Rev. Lett. **94**, 025901 (2005).
[6] S. P. Jang and S. Choi, Appl. Phys. Lett. **84**, 4316 (2004).
[7] J. C. Maxwell, *A Treatise on Electricity and Magnetism, II Edition* (Clarendon, Oxford, 1881).
[8] S. A. Putnam, D. G. Cahill, P. V. Braun, Z. Ge, and R. G. Shimm, J. Appl. Phys. **99**, 084308 (2006).
[9] J. Eapen, W. C. Williams, J. Buongiorno, L. W. Hu, S. Yip, R. Rusconi, and R. Piazza, Phys. Rev. Lett. **99**, 095901 (2007).
[10] M. Vladkov and J.-L. Barrat, Nano Lett. **6**, 1224 (2006).
[11] S. Krishnamurthy, P. Bhattacharya, P. Phelan, and R. Prasher, Nano Lett. **6**, 419 (2006).
[12] H. Zhu, C. Zhang, S. Liu, Y. Tang, and Y. Yin, Appl. Phys. Lett. **89**, 023123 (2006).
[13] E. V. Timofeeva, A. N. Gavrilov, J. M. McCloskey, Y. V. Tolmachev, S. Sprunt, L. M. Lopatina, and J. V. Selinger, Phys. Rev. E **76**, 061203 (2007).
[14] C. H. Li, W. Williams, J. Buongiorno, Lin-Wen. Hu, and G. P. Peterson, ASME J. Heat Transfer **130**, 042407 (2008).
[15] R. Prasher, W. Evans, P. Meakin, J. Fish, P. Phelan, and P. Keblinski, Appl. Phys. Lett. **89**, 143119 (2006); W. Evans, R. Prasher, J. Fish, P. Meakin, P. Phelan, and P. Keblinski, Int. J. Heat Mass Transfer **51**, 1431 (2008).
[16] N. R. Karthikeyan, J. Philip, and B. Raj, Mater. Chem. Phys. **109**, 50 (2008).
[17] R. Prasher, P. Phelan, and P. Bhattacharya, Nano Lett. **6**, 1529 (2006).
[18] P. G. Klemens, High Temp. - High Press. **23**, 241 (1991).
[19] B. Shafiro and M. Kachanov, J. Appl. Phys. **87**, 8561 (2000).
[20] Z. Wang, A. Kulkarni, S. Deshpande, T. Nakamura, and H. Herman, Acta Mater. **51**, 5319 (2003).
[21] L. Braginsky, V. Shklover, G. Witz, and H.-P. Bossmann, Phys. Rev. B **75**, 094301 (2007).
[22] J. Berryman, Appl. Phys. Lett. **86**, 032905 (2005); J. Appl. Phys. **97**, 063504 (2005).
[23] M. Vladkov and J.-L. Barrat, J. Comput. Theor. Nanosci. **5**, 187 (2008).
[24] C.-W. Nan, R. Berringer, D. Clark, and H. Gleiter, J. Appl. Phys. **81**, 6692 (1997).
[25] J. A. Eastman, S. R. Phillpot, S. U. S. Choi, and P. Keblinski, Annu. Rev. Mater. Res. **34**, 219 (2004).
[26] W. Yu and S. U. S. Choi, J. Nanopart. Res. **5**, 167 (2003); **6**, 355 (2004).
[27] L. Xue, P. Keblinski, S. R. Phillpot, S. U.-S. Choi, and J. A. Eastman, Int. J. Heat Mass Transfer **47**, 4277 (2004).
[28] J. A. Greathouse and D. A. McQuarrie, J. Colloid Interface Sci. **181**, 319 (1996).
[29] N.-K. Lee and T. A. Vilgis, Eur. Phys. J. B **28**, 451 (2002).
[30] I. Park, Z. Li, A. P. Pisano, and R. S. Williams, Nano Lett. **7**, 3106 (2007).